Experimental evidence of the crucial role of nonmagnetic Pb cations in the enhancement of the Néel temperature in perovskite $Pb_{1-x}Ba_xFe_{1/2}Nb_{1/2}O_3$

I. P. Raevski, S. P. Kubrin, S. I. Raevskaya, V. V. Titov, D. A. Sarychev, M. A. Malitskaya, I. N. Zakharchenko, and S. A. Prosandeev*

Department of Physics, Institute of Physics, Southern Federal University, Rostov on Don 344090, Russia

(Received 4 June 2009; revised manuscript received 14 June 2009; published 10 July 2009)

Our experimental study of $Pb_{1-x}Ba_xFe_{1/2}Nb_{1/2}O_3$ shows that, the Néel temperature in this solid solution drops down at $x \approx 0.15/0.20$, and, at the same threshold, the polarization also looses its long-range order. Thus, the multifunctional solid solution studied demonstrates a possibility of *simultaneous* controlling the magnetic and ferroelectric properties by changing the concentration of only lead, which is a nonmagnetic ion.

DOI: 10.1103/PhysRevB.80.024108 PACS number(s): 77.22.Ch, 75.50.Ee, 75.30.Et, 76.80.+y

I. INTRODUCTION

Multiferroics are currently in the focus of the material science[1,2] and the list of the multiferroics is constantly updated. One of the promising examples $Pb(Fe_{1/2}Nb_{1/2})O_3$ (PFN)[3] has a perovskite ABO_3 structure with a quite random occupation of the B site by Fe and Nb. The rhombohedral and monoclinic structures belonging to the $R3m$ and Cm space groups, respectively, have been reported for the room-temperature phase of PFN in several independent studies (see, e.g., Refs. 4 and 5, and references therein). The ferroelectric phase transition in PFN happens at about 380 K. As in other similar lead-free $A^{2+}Fe_{1/2}B^{5+}_{1/2}O_3$ perovskites (A^{2+}=Ba,Sr,Ca, B^{5+}=Nb,Ta),[6,7] the ground magnetic state of PFN appears to be spin glass,[5] below ~20 K. However, in contrast to its lead-free counterparts, PFN exhibits also a long-range G-type antiferromagnetic (AFM) order with a much higher Néel temperature,[1–5] $T_N \approx 150$ K. The AFM phase transition in PFN is manifested by anomalies in the temperature dependence of the dielectric permittivity[8] and lattice parameters.[4] The nature of the strong enhancement of T_N in PFN is not clear, and, in this paper, we state the question how one could control this temperature in other way than trivial changing in the Fe content. We suggest diluting PFN with $Ba(Fe_{1/2}Nb_{1/2})O_3$, which does not possess Pb, and we experimentally show that T_N (as well as the ferroelectric phase-transition temperature) are very sensitive to the substitutions in the Pb sublattice. Possible nature of this sensitivity is also discussed.

The structure of the paper is as follows. At the beginning, we describe the experimental methods in use and characterization of the samples obtained. Then we report on our findings for the Néel temperature dependence on the composition. Theoretical description and discussion of the results obtained follows the description of the experiment. We continue with analyzing the ferroelectric properties in the same samples and finally we come to our conclusions.

II. EXPERIMENTAL

Ceramic samples of $Pb_{1-x}Ba_xFe_{1/2}Nb_{1/2}O_3$ (PBFN) with $0 \le x \le 0.30$ have been obtained by the solid-state reaction route using high-purity Fe_2O_3, Nb_2O_5, PbO, and $BaCO_3$. These ingredients were batched in stoichiometric proportions and 1 wt % Li_2CO_3 was added to the batch. This addition promotes the formation of the perovskite modification of PFN and reduces its conductivity significantly.[9] For the sake of comparison, we synthesized also the $Pb_{1/2}Ca_{1/2}(Fe_{1/2}Nb_{1/2})O_3$ composition and some PBFN compositions without Li_2CO_3 additions. After thorough mixing of the powders in an agate mortar with ethyl alcohol and subsequent drying, green samples were pressed at 100 MPa in the form of disks of 10 mm in diameter and of 2–4 mm in height using polyvinyl alcohol as a binder. Sintering was performed at 1050–1100 °C for 2 h in a closed alumina crucible. The density of the obtained ceramics was about 90–95% of theoretical one. The electrodes for measurements were deposited to the grinded disks of 9 mm in diameter and 0.9 mm in height by firing on silver past. The preparation of $A^{2+}Fe_{1/2}B^{5+}_{1/2}O_3$ ceramic samples (A^{2+}=Ba,Sr,Ca, B^{5+}=Nb,Sb) as well as the details of the dielectric and Mössbauer studies have been described elsewhere.[10,11] To characterize the samples, we performed x-ray diffraction studies by using DRON-7 diffractometer with Co Kα radiation.

III. RESULTS

All of the investigated compositions were single phase and had a structure of the perovskite type. PFN had rhombohedral symmetry at room temperature while the PBFN compositions with $0.05 \le x \le 1.0$ were cubic. We found that the concentration dependence of the pseudocubic lattice parameter $\tilde{a}=V^{1/3}$ is pretty linear, that is, a sign of the formation of solid solutions in the whole concentration range [Fig. 1(a)].

Figure 2 shows the temperature dependence of the dielectric permittivity ε for some PBFN compositions studied. On the basis of these data we found that the ferroelectric phase-transition temperature decreases approximately linearly with x in the interval of the concentrations between 0 and 0.2 [Fig. 1(a)]. Above this concentration, the permittivity becomes rather dispersive and the inherent to relaxor ferroelectrics Vogel-Fulcher law[12] fits well the experimental frequency dependence of the $\varepsilon(T)$ maximum temperature T_m. PBFN with $x=1$ (BFN) exhibits a steplike $\varepsilon(T)$ dependence and very high (about 20 000) values of permittivity. Both these features as well as a Debye-type dispersion are the fingerprints of the Maxwell-Wagner relaxation as was discussed in detail elsewhere.[10]

At room temperature, the Mössbauer ^{57}Fe spectra of all studied compositions are doublets with the quadrupole split-

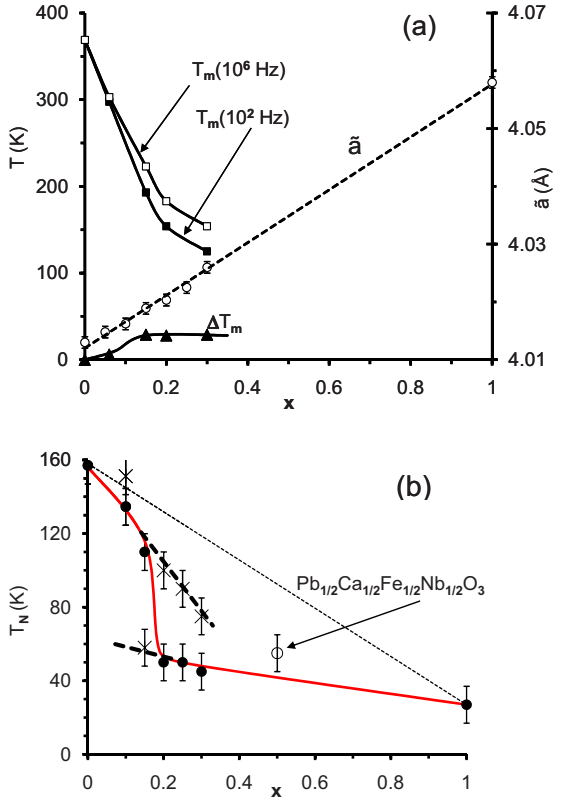

FIG. 1. (Color online) Concentration dependence of (a) the dielectric-permittivity maximum temperature T_m, pseudocubic lattice parameter $\tilde{a}=V^{1/3}$, frequency shift $\Delta T_m=T_m(10^6$ Hz$)-T_m(10^2$ Hz) and (b) Néel temperature T_N for PBFN solid solutions. Circles and crosses in Fig. 1(b) correspond to T_N values determined from the main and additional anomalies of $\eta(T)$ dependences shown in the inset of Fig. 2.

ting of ≈0.4 mm/s and isomer shift of 0.4 mm/s (relative to metallic iron). Incomplete ordering of the Fe^{3+} and Nb^{5+} ions in the lattice of PBFN is believed to be the main cause of this quadrupole splitting.[6,13] In contrast to this, in the fully (long-range) 1:1 (NaCl-type) ordered structure, one can expect the presence of only one peak in the Mössbauer spectra. Such a situation takes place in $A(Fe_{1/2}Sb_{1/2})O_3(A=Ca,Sr,Pb)$ perovskites, where a high degree of ordering is confirmed by the appearance of the superstructural reflections on x-ray diffractogramms.[6,13]

When decreasing temperature below T_N, the Mössbauer spectrum transforms from doublet to sextet.[6,7,9,13] This transformation is accompanied by a strong decrease in the magnitude η of the γ absorption normalized to its value at 300 K (see the inset in Fig. 2). The abrupt drop in the temperature dependence of η allows one to determine T_N from the Mössbauer experiment.[11] We used this possibility and experimentally found T_N in PBFN [Fig. 1(b)] and some $A^{2+}Fe_{1/2}B^{5+}_{1/2}O_3$ perovskites ($A^{2+}=Ba,Sr,Ca$, $B^{5+}=Nb,Sb$). The results for the latter compounds agree well with the data obtained from the magnetic-susceptibility measurements.[6,7] No valuable effect of Li_2CO_3 addition on the magnetic or ferroelectric phase-transition temperatures has been observed for the sintering conditions used. One can see that, in PBFN, at small Ba concentrations (below $x\approx0.2$), T_N linearly decreases but

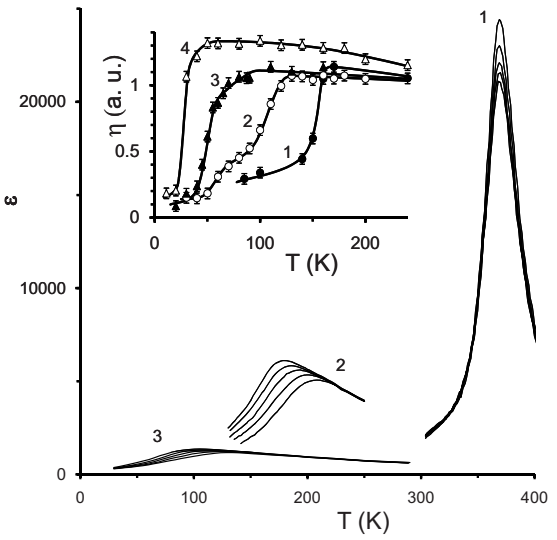

FIG. 2. Temperature dependence of permittivity ε for some PBFN ceramic compositions measured at different frequencies: 10^2, 10^3, 10^4, 10^5, and 10^6 Hz (from top to bottom). The inset shows the temperature dependence of the η-maximal value of the absorption in the Mössbauer spectrum related to its value at 300 K, for some PBFN compositions. (1) $x=0$; (2) $x=0.15$; (3) $x=0.30$; and (4) $x=1.0$.

keeps having large values of about 100–150 K. At $x\approx0.2$, T_N abruptly falls down to smaller values of ~50 K. Close to this drop down, additional $\eta(T)$ anomalies inherent to phase coexistence were observed (inset in Fig. 2). The corresponding values of T_N are shown in Fig. 1(b) with dashed lines. Pure BFN has $T_N\approx25$ K, in good agreement with the magnetic-susceptibility measurements.[6,7] Thus, all data obtained for T_N is split into two different sets. One is at 100–150 K. The other is at 30–50 K. We assign these two sets to two different magnetic order parameters. It is interesting that, at $x\approx0.2$, these two temperature sets coexist which can imply the coexistence of the two order parameters (via metastable states). Below, we will discuss possible nature of these two parameters.

IV. DISCUSSION AND CONCLUSION

The AFM order in iron oxides is usually attributed[14] to the oxygen-related superexchange Fe^{3+}-O-Fe^{3+}. The same mechanism is supposed to work in perovskites.[1,15] However, the number of the Fe^{3+}-O-Fe^{3+} pairs determining T_N does not change in PBFN when varying x but the experimentally obtained values of T_N change a lot. In principle, there can be some indirect changes in the oxygen-related superexchange via the change in the excitation energy between the oxygen and iron electron energy levels, as well as because of possible change in the hopping integral between these states via (i) possible change in the degree of the Fe and Nb order, (ii) the change in the lattice parameter, or (iii) a dramatic (to nanolevel) decrease in the grain size. However, (i) our Mössbauer, dielectric, and x-ray studies do not show any evidence of the change in the degree of the Fe and Nb cations ordering in PBFN. In the case of the long-range ordering one would

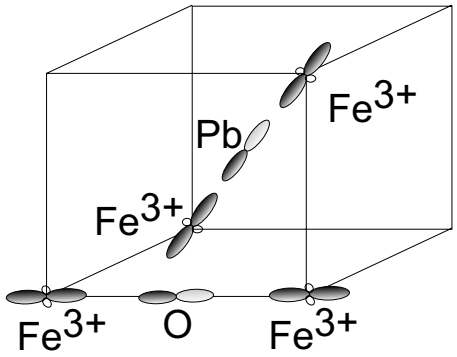

FIG. 3. Schematic plot of the superexchange via Pb and oxygen.

see a singlet component in the Mössbauer spectra or superstructural lines in the x-ray diffraction pattern or strong decrease in the frequency dispersion of the permittivity maximum. None of these features has been observed. This implies that the change in the degree of ordering is not behind the observed change in T_N in PBFN. (ii) We measured T_N in $Pb_{1/2}Ca_{1/2}(Fe_{1/2}Nb_{1/2})O_3$($\bar{a}$=3.948 Å) and found that T_N in this solid solution is close to the values obtained for the corresponding PBFN compositions, in spite of a big difference in the lattice constant. Thus, the change in the lattice constant cannot be responsible for the strong change in T_N in PBFN. (iii) Our studies of the grain structure of the ceramics revealed that the mean grain size of PBFN ceramics does not change substantially with x and is about 3–10 μm. We conclude that the change in the size of the grains with x does not control the observed change in T_N in PBFN. Thus, the weird enhancement of T_N in PFN does not have a simple explanation. Below, we discuss this challenge from the point of view of possible leading role of Pb in the both magnetic and ferroelectric couplings. The ferroelectric coupling in the Pb-containing perovskites is usually enhanced owing to the strong ferroelectric activity of Pb.[16] The magnetic coupling can be enhanced either because of the involvement of the Pb ions into the superexchange or because of the influence of the Pb-related polarization onto the magnetic properties.

We start here from the discussion of the first alternative, the possible involvement of the Pb ions into the superexchange. In the framework of this assumption, at low x, the magnetic interactions in PBFN can percolate via the Pb sublattice and can organize a long-range AFM order. The linear decrease in T_N with x seen in Fig. 1(b), at low x, can be explained within this framework by the decreasing number of the Fe^{3+}-Pb-Fe^{3+} pairs. The abrupt drop in T_N can be explained now as the result of the loss of the percolation of the AFM order in the Fe sublattice. Notice that the comparatively low value of the percolation threshold can be a result of the contribution to the superexchange from the second- and third-neighbor's interactions.[17]

Let us briefly discuss possible models for such unusual superexchange. We start from the possibility that the Pb $6p\sigma$ orbitals can connect the nearest neighbors of Fe's in the [111] direction (Fig. 3). These pairs are so-called third neighbors (the first neighbors are in the [001] directions and are coupled via oxygen and the second neighbors are in the [110] direction). The effective Pb-related superexchange can be expressed now by using the fourth-order quantum perturbation theory, over the hopping integral between the Pb and Fe sites t_A, the energy difference between the states on Fe and Pb Δ_A, and the Coulomb integral on the Fe (Pb) site $U(U_A)$ (see Appendix),

$$J_A = \frac{2t_A^4}{\Delta_A^2}\left(\frac{1}{U} + \frac{2}{2\Delta_A + U_A}\right). \quad (1)$$

Theoretical estimation of the magnitude of this coupling is not known at present. However, the real coupling might be more complicated and involve the jumps via oxygens. Indeed, the t_{PbO} Pb-Oσ hopping integral was found to have a large value of 0.9 eV.[18] Additionally, experimental results on conductivity and photoconductivity[19] revealed the fact that lead-containing perovskites have band gaps strongly smaller compared with the gap in the corresponding lead-free perovskites, and this gap is due to the electron excitation between O $2p$ and Pb $6p$ states. One should also take into account the fact that each oxygen ion has four nearest Pb ions. Then the probability of the hopping of an electron between oxygen ions via lead can get a value sufficient for coupling nearest broken iron bonds (cf. Ref. 20). For instance, if one takes the O $2p$ to Pb $6p$ excitation energy 2.5 eV, then the maximal Pb-related magnetic energy can be estimated as $4[4(0.9/2.5)^4]=0.26$ of the energy of the superexchange via oxygen. If we take for reference T_N=640 K in $BiFeO_3$ then the magnetic energy related to Pb will be $640\times0.26=166$ K. This value is in line with the known T_N value of PFN. Thus, lead can serve as a mediator between the local AFM clusters.

It is surprising that the T_N of 150 K assigned to the superexchange via Pb is several times larger than T_N of 25 K, which in lead-free perovskites can be assigned to oxygen only. We relate this fact to the glass behavior in the lead-free perovskites such as BFN. Correspondingly, in these perovskites, there are only small and *dynamical* AFM clusters, which do not percolate magnetic interactions, due to broken bonds and random fields.[21] It has been believed that only those Fe ions contribute to the antiferromagnetic interactions, which have more than one bridge.[14] So, many iron ions are at the surface of the magnetic clusters and do not take a part in the magnetism of the lead-free perovskites. At short distances, the Fe and Nb ions can have a rather strong (NaCl-type 1:1) order preventing the superexchange via oxygen. This can happen owing to the Coulomb interactions between Fe^{3+} and Nb^{5+}, when growing the crystals or sintering ceramics. The occupation of the third neighbors by Fe and Nb can be less correlated (compared to the first neighbors) and, consequently, the probability to find a pair of Fe's coupled by Pb is larger than the probability to find two Fe's coupled by oxygen because Pb couples third neighbors. In contrast to this, if the (FeNb) sublattice is well ordered,[13] like in $Pb(Fe_{1/2}Sb_{1/2})O_3$, then even Pb cannot increase T_N, and T_N is of about 25 K. Thus, Pb can merge the magnetic moments of the small random and dynamical magnetic clusters in PFN, which are not well ordered, and this can result in the percolation of the AFM interactions through the lattice. Notice that

even in pure PFN there remains a lot of uncoupled dynamical magnetic clusters leading to the spin glass formation below ≈20 K.[5] This point is in line with our experiment and theory predicting the coexistence of the two magnetic order parameters at low temperatures, the first-order parameter is related to the superexchange via Pb while the second order parameter has the origin in the O-related superexchange.

Let us now turn to the dielectric properties of PFN. Notice that the importance of Pb for the lattice dynamics (and consequently for ferroelectricity) in PFN follows from our results of first-principles computations, which revealed the presence of the soft ferroelectric mode consisting of a polar displacement of the Pb ions opposite to the shift in the other ions (mostly oxygen ions).[22] Hence, one can expect that the dilution of the Pb sublattice should result in diminishing the ferroelectric properties inherent to pure PFN. Indeed, as one can see from Figs. 1(a) and 2, the dielectric properties substantially change at the threshold concentration $x \approx 0.15-0.2$, which is close to the threshold obtained by studying the magnetic properties. Below this concentration, the dielectric-permittivity maximum is large and the frequency dispersion is small that can mean that the Pb-related network mostly defining the ferroelectric properties is homogeneous and macroscopic (percolative), and the lattice dynamics is soft-mode related. Above this concentration, there appears a strong dispersion inherent to relaxors, the source of which is usually associated with finite-size Pb-related polar regions. The start of the strong frequency dispersion, thus, manifests the prevalence of the relaxation dielectric response in the inhomogeneous ferroelectric over the mean-field, homogeneous soft-mode-related response. This evidence is in excellent agreement with recent experimental observation of the coexistence of the magnetic and ferroelectric glass states[2] in $(Sr,Mn)TiO_3$. Indeed, our data show that, above $x=0.2$, in PBFN, ferroelectric relaxor behavior coexists with the magnetic glass state inherent to lead-free double perovskites.[6,7] We should emphasize, at the same time, that our studies show the relaxor and magnetic glass behavior because of diluting a ferroelectrically active ion Pb, while Ref. 2 reports about doping $SrTiO_3$ with magnetically active cation Mn.

The proximity of the ferroelectric and long-range AFM thresholds can be not occasional, but rather this can manifest whether a strong influence of the ferroelectric polar distortions on T_N via the oxygen-related superexchange or/and be a result of the existence of the straight Pb-related superexchange described in the present paper. Both factors lead to the same conclusion, a possibility to control both the ferroelectric and AFM properties of PFN by diluting the Pb sublattice.

ACKNOWLEDGMENTS

The authors appreciate discussions with Jak Chakhalian, V. P. Sakhnenko, and R. V. Vedrinskii. This study is supported by the Russian Foundation for Basic Research (RFBR) under Grants No. 08-02-92006 NNS, No. 07-02-00099, and No. 09-02-92672 IND.

APPENDIX

1. The fourth-order contribution to the energy

The idea of the derivation is to use the quantum theory of perturbations in order to calculate the energy of the ferromagnetically and AFM-ordered spins. The contributions to the first, second, and third order are the same for these two types of ordering and we omit consideration of these terms. Thus, we start from the contribution, which is distinct for the ferromagnetic and antiferromagnetic orders. The general formula for this contribution reads,

$$E^{(4)} = -\sum \frac{\langle 0|H|i\rangle\langle i|H|j\rangle\langle j|H|k\rangle\langle k|H|0\rangle}{(E_i - E_0)(E_j - E_0)(E_k - E_0)}. \quad \text{(A1)}$$

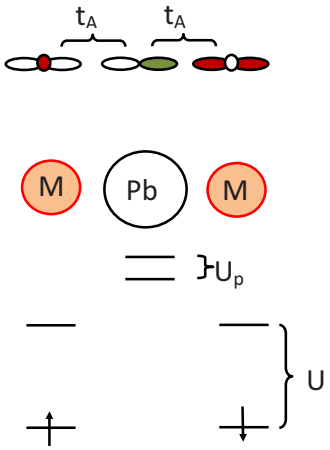

FIG. 4. (Color online) Two-electron-three-site model.

2. Two-electron-three-site model

Consider a Pb ion sandwiched between two metal sites (Fig. 4). Each metal site has one orbital and it can accept one or two electrons with opposite spins. The $6p$ Pb orbital is empty in the ground state (it is directed toward the metals) and can accept up to two electrons with opposite spins. The Ms each have an orbital directed toward Pb. The hopping integral between the nearest sites is t_A. The splitting of the levels on M is U. The splitting of the levels on Pb is U_p. The ground state includes one electron on the left M and one electron on the right M. The spins of the electrons are to be determined on the basis of energy minimization.

3. Hamiltonian matrix including the excitations from *M* to Pb

We want to find the energy of the ground state with taking into account the covalency-mediated electron excitations (Fig. 5). The first virtual excitation from M to Pb has energy Δ_A. The followed virtual excitation of the other electron from the second M to Pb gives the energy $2\Delta_A + U_p$, where U_p is the Coulomb interaction energy of two electrons on the Pb site (Table I).

In the case of ferromagnetic ground state, the virtual excitation of two electrons on Pb is not possible because of the Pauli principle. For the AFM ground state, the numerator in formula (A1) will have the product of all the finite nondiagonal elements in the matrix. The denominator will include the product of Δ_A (two times because we pass this state two times in the virtual excitation and in the de-excitation) and $2\Delta_A + U_p$. We add to this formula factor 4 because there are four ways how to excite two electrons from two metals to Pb

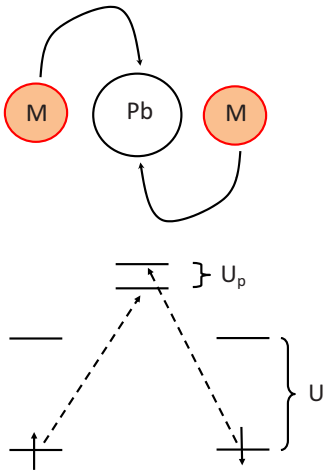

FIG. 5. (Color online) Superexchange via Pb $6p$ empty state—excitation of both electrons on lead.

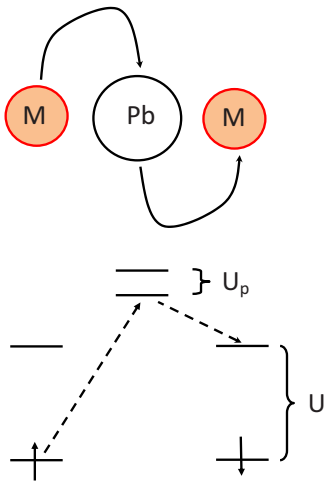

FIG. 6. (Color online) Superexchange via Pb $6p$ empty state—excitation of an electron from one metal ion to the other one.

and how to come back (one has the choice to excite whether the left or right M, first. Then, when two electrons are on Pb, one has a choice whether to return an electron to the left or right M, first).

$$E_{\uparrow\uparrow} = 0, \tag{A2}$$

$$E_{\uparrow\downarrow} = -\frac{4t_A^4}{\Delta_A^2}\frac{1}{2\Delta_A + U_p}. \tag{A3}$$

4. Hamiltonian matrix including excitations from one M to the other via Pb

The first virtual excitation from a metal to Pb has energy Δ_A. The virtual excitation of the same electron from Pb to the other M has energy U, where U is the Coulomb interaction energy of two electrons on the M site (Fig. 6).

In the case of ferromagnetic ground state, the virtual excitation of an electron from one M to the other, via Pb, is forbidden by the Pauli principle. For the AFM ground state, the numerator in formula (A1) will have the product of all finite nondiagonal elements in the matrix. The denominator will include the product of Δ_A (two times, because we pass this state two times, in the virtual excitation and in the de-excitation) and U. We add to this formula factor 2 because there are two ways how to excite an electron from one metal to the other via Pb (one has the choice to excite whether the left or right M, first) (Table II).

$$E_{\uparrow\uparrow} = 0, \tag{A4}$$

$$E_{\uparrow\downarrow} = -\frac{2t_A^4}{\Delta_A^2 U}. \tag{A5}$$

5. Final formula

The difference between the energy of the AFM and ferromagnetic states gives the value of the indirect interaction energy between the spins (notice that another definition will result in a factor in our expression)

$$J_A = -\frac{4t_A^4}{\Delta_A^2}\frac{1}{2\Delta_A + U_p} - \frac{2t_A^4}{\Delta_A^2 U} = -\frac{2t_A^4}{\Delta_A^2}\left(\frac{1}{U} + \frac{2}{2\Delta_A + U_p}\right). \tag{A6}$$

Formally, this result coincides with the formula known for the superexchange energy in the M-O-M fragment, where O is oxygen. This formula can be obtained in a four-electrons-three-sites model.[23–30] This coincidence is not accidental. Indeed, the four-electron model gives the same results as a two-hole model and the two-hole model has formally the same energy spectrum in the considered case as two-electron model. Indeed, in the electron representation, d^5 shell transforms again to a d^5 shell but in the hole representation. Thus, there is isomorphism between the Anderson four-electron-three-site model and considered above two-electron-three-site model. However, one should remember about very different meaning of the parameters in our model compared to the Anderson model.

TABLE I. Hamiltonian matrix including the excitations from M to Pb.

$2\Delta_A + U_p$	t_A	0
t_A	Δ_A	t_A
0	t_A	0

TABLE II. Hamiltonian matrix including excitations from one M to the other via Pb.

U	t_A	0
t_A	Δ_A	t_A
0	t_A	0

*Also at Physics Department, University of Arkansas, Fayetteville, Arkansas 72701.

[1] V. A. Bokov, I. E. Myl'nikova, and G. A. Smolenkii, Sov. Phys. JETP **15**, 447 (1962).

[2] V. V. Shvartsman, S. Bedanta, P. Borisov, W. Kleemann, A. Tkach, and P. M. Vilarinho, Phys. Rev. Lett. **101**, 165704 (2008).

[3] A. Levstik, C. Filipič, and J. Holc, J. Appl. Phys. **103**, 066106 (2008).

[4] S. P. Singh, D. Pandey, S. Yoon, S. Baik, and N. Shin, Appl. Phys. Lett. **90**, 242915 (2007).

[5] G. M. Rotaru, B. Roessli, A. Amato, S. N. Gvasaliya, C. Mudry, S. G. Lushnikov, and T. A. Shaplygina, Phys. Rev. B **79**, 184430 (2009).

[6] P. D. Battle, T. C. Gibb, A. J. Herod, S.-H. Kim, and P. H. Munns, J. Mater. Chem. **5**, 865 (1995).

[7] K. Tezuka, K. Henmi, Y. Hinatsu, and N. M. Masaki, J. Solid State Chem. **154**, 591 (2000).

[8] Y. Yang, J.-M. Liu, H. B. Huang, W. Q. Zou, P. Bao, and Z. G. Liu, Phys. Rev. B **70**, 132101 (2004).

[9] I. P. Rayevsky, A. A. Bokov, A. S. Bogatin, S. M. Emelyanov, M. A. Malitskaya, and O. I. Prokopalo, Ferroelectrics **126**, 191 (1992).

[10] I. P. Raevski, S. A. Prosandeev, A. S. Bogatin, M. A. Malitskaya, and L. Jastrabik, J. Appl. Phys. **93**, 4130 (2003).

[11] I. P. Raevski, S. P. Kubrin, S. I. Raevskaya, V. V. Stashenko, D. A. Sarychev, M. A. Malitskaya, M. A. Seredkina, V. G. Smotrakov, I. N. Zakharchenko, and V. V. Eremkin, Ferroelectrics **373**, 121 (2008).

[12] F. Chu, I. M. Reaney, and N. Setter, Ferroelectrics **151**, 343 (1994).

[13] I. P. Raevskii, D. A. Sarychev, S. A. Bryugeman, L. A. Reznichenko, L. A. Shilkina, O. N. Razumovskaya, V. S. Nikolaev, N. P. Vyshatko, and A. N. Salak, Crystallogr. Rep. **47**, 1012 (2002).

[14] M. A. Gilleo, J. Phys. Chem. Solids **13**, 33 (1960).

[15] S. Nomura, H. Takabayashi, and T. Nakagawa, Jpn. J. Appl. Phys. **7**, 600 (1968).

[16] R. Cohen, Nature (London) **358**, 136 (1992).

[17] G. E. Pike and C. H. Seager, Phys. Rev. B **10**, 1421 (1974).

[18] S. A. Prosandeev, Y. Y. Tarasevich, and N. M. Teslenko, Ferroelectrics **131**, 137 (1992).

[19] I. P. Raevskii, S. A. Prosandeev, and I. A. Osipenko, Phys. Status Solidi B **198**, 695 (1996).

[20] K. Foyevtsova, R. Valentí, and P. J. Hirschfeld, Phys. Rev. B **79**, 144424 (2009).

[21] R. Rodriguez, A. Fernandez, A. Isalgue, J. Rodrigez, A. Labarta, J. Tejada, and X. Obrador, J. Phys. C **18**, L401 (1985).

[22] R. Demirbilek, A. V. Kutsenko, S. Kapphan, I. Raevski, S. Prosandeev, B. Burton, L. Jastrabik, and V. Vikhnin, Ferroelectrics **302**, 279 (2004).

[23] P. W. Anderson, Phys. Rev. **79**, 350 (1950).

[24] J. B. Goodenough, Phys. Rev. **100**, 564 (1955).

[25] J. B. Goodenough, *Magnetism and Chemical Bond* (Interscience-Wiley, New York, 1963).

[26] J. Kanamori, J. Phys. Chem. Solids **10**, 87 (1959).

[27] K. I. Kugel and D. I. Khomskii, Sov. Phys. JETP **37**, 725 (1973).

[28] H. Eskes and J. H. Jefferson, Phys. Rev. B **48**, 9788 (1993).

[29] D. Khomskii, Lect. Notes Phys. **569**, 89 (2001).

[30] A. I. Lichtenshtein, *Schriften des Forschungszentrums Jülich*, Series Matter and Materials, Vol. 26 (Springer, Jülich, 2005), pp. A7.1–36.